A. Duarte-Ruiz[1,*], H. Iuele[1,2], S. A. Torres-Cortés[1], A. Meléndez[1], J. D. Velásquez[3], M. N. Chaur[3,4]

[1]Departamento de Química, Universidad Nacional de Colombia. Sede Bogotá, Cra. 30 No. 45-02, Bogotá-Colombia.
[2]Institute of Nanotechnology, National Research Council (CNR-NANOTEC), Via Monteroni, Lecce-Italy.
[3]Departamento de Química, Universidad del Valle, A.A. 25360, Santiago de Cali-Colombia
[4]Centro de Excelencia en Nuevos Materiales (CENM), Universidad del Valle, A.A. 25360, Santiago de Cali-Colombia

***Correspondig author:** aduarter@unal.edu.co

Received: 23/06/2020. Last review: 13/07/2020. Approved: 26/08/2020.

Physical and Inorganic Chemistry

Synthesis and characterization of C_{60} and C_{70} acetylacetone monoadducts and study of their photochemical properties for potential application in solar cells

Abstract

We report on the synthesis of C_{60} and C_{70} monoadducts at room temperature through the Bingel reaction; employing acetylacetone as ligand; in presence of DBU (1,8-Diazabicyclo [5.4.0] undec-7-ene), carbon tetrabromide (CBr_4), and o-dichlorobenzene. Diacetylmethane-[C_{60}-I_h]-fullerene-[5,6] and diacetylmethane-[C_{70}-D_{5h}]-fullerene-[5,6] monoadducts were obtained with yields of 69% and 44%, respectively. The products were purified by column chromatography (CC, on silica gel, using hexane, carbon disulfide, and chloroform as eluents at room temperature) and characterized by Nuclear Magnetic Resonance (^{1}H and ^{13}C), Fourier-Transform Infrared (FT-IR) and UV-Visible spectroscopies, Matrix-assisted Laser Desorption/Ionization-Time of Flight (MALDI-TOF) Mass spectrometry, Cyclic Voltammetry (CV), and Osteryoung Square Wave Voltammetry (OSWV). Both compounds showed irreversible reduction peaks controlled by diffusion, with LUMO energy levels of -3.09 eV, -3.13 eV for C60, and C_{70} monoadducts, respectively. These values are comparable with the -3.99 eV of PC61BM. The synthetized adducts were incorporated into inverted-type perovskite solar cells and were used as electron transporting materials (ETM) obtaining power conversion efficiencies (PCE) of 8.5% and 14.0% for the C_{60} and C_{70} monoadducts, respectively. When C_{60} is replaced by a lower symmetrical fullerene such as C_{70} an improved light absorption in the visible region is observed.

Keywords: Fullerenes; Bingel reaction; acetylacetone; perovskite; solar cells.

Síntesis y caracterización de monoaductos de C_{60} y C_{70} con acetilacetona y estudio de sus propiedades fotoquímicas para su posible aplicación en células solares

Resumen

Reportamos la síntesis de monoadductos de C_{60} y C_{70} a temperatura ambiente a través de la reacción de Bingel, empleando acetilacetona como ligando, en presencia de DBU (1,8-diazabiciclo [5.4.0] undec-7-eno), tetrabromuro de carbono (CBr_4) y o-diclorobenceno. Se obtuvieron monoadductos de diacetilmetano-[C_{60}-I_h]-fullereno-[5,6] y diacetilmetano-[C_{70}-D_{5h}]-fullereno-[5,6] con rendimientos del 69% y 44%, respectivamente. Los productos se purificaron por cromatografía en columna (CC, usando silica gel, hexano, disulfuro de carbono y cloroformo como fase móvil, a temperatura ambiente) y se caracterizaron por resonancia magnética nuclear (^{1}H y ^{13}C), infrarrojo con transformada de Fourier (FT-IR), espectroscopia UV-Visible, espectrometría de masas, desorción/ionización láser asistida por matriz - tiempo de vuelo (MALDI-TOF), voltametría cíclica (CV) y voltametría de onda cuadrada de Osteryoung (OSWV). Ambos compuestos mostraron picos de reducción irreversibles controlados por difusión, con niveles de energía LUMO de -3,09 eV y -3,13 eV para los monoadductos C_{60} y C_{70}, respectivamente. Estos valores son comparables con el -3,99 eV de PC61BM. Los aductos sintetizados se incorporaron a las células solares de perovskita de tipo inversa y se usaron como materiales de transporte de electrones (ETM) obteniendo eficiencias de conversión de energía (PCE) de 8,5% y 14,0% para los monoaductos C_{60} y C_{70}, respectivamente. Cuando el C60 se reemplaza por un fullereno menos simétrico como el C_{70}, se observa una absorción de luz mejorada en la región visible.

Palabras clave: fullerenos; reaccion Bingel; acetilacetona; perovskita, celdas solares.

Sínteses e caracterização de monoadutos de C_{60} e C_{70} com acetilacetona e estudo das suas propriedades fotoquímicas para a sua possível aplicação em células solares

Resumo

Reportamos a sínteses de monoadutos de C60 e C_{70} a temperatura ambiente através da reação de Bingel, utilizando acetilacetona como ligando, na presença de DBU (1,8-diazabiciclo [5.4.0] undec-7-eno), tetrabromuro de carbono (CBr_4) e o-diclorobenzeno. Foram obtidos monoadutos de diacetilmetano-[C60-I_h]-fulereno-[5,6] e diacetilmetano-[C_{70}-D_{5h}]-fulereno-[5,6] com rendimentos de 69% e 44%, respectivamente. Os produtos se purificaram por cromatografia em coluna (CC, usando sílica gel, hexano, dissulfeto de carbono e clorofórmio como fase móvel à temperatura ambiente) e se caracterizaram por ressonância magnética nuclear (^{1}H e ^{13}C), infra-vermelho com transformada de Fourier (FT-IR), espectroscopia UV-Visível, espectrometria de massas, ionização e dessorção a laser assistida por matriz-tempo de voo (MALDI-TOF), voltametria cíclica (CV) e voltametria de onda quadrada de Osteryoung (OSWV). Ambos compostos mostraram picos de redução irreversíveis controlados por difusão, com níveis de energia LUMO de -3,09 eV, -3,13 eV para os monoadutos C_{60} e C_{70}, respectivamente. Estos valores são compráveis com -3,99 eV de PC61BM. Os adutos sintetizados se incorporaram nas células solares de perovskita de tipo inversa e se usaram como materiais de transporte de eletrões (ETM) obtendo eficiências de conversão de energia (PCE) de 8,5% e 14,0% para os monoadutos C_{60} e C_{70}, respectivamente. Quando o C_{60} se substitui por um fulereno menos simétrico como o C_{70}, se observa uma absorção de luz melhorado na região visível.

Palavras-chave: fulerenos; reação Bingel; acetilacetona; perovskita, células solares.

Introduction

Fullerenes are a family of molecules that own a highly symmetric closed cage structure, exclusively made up of carbon atoms. Unlike the other allotropic forms of carbon, such as diamond and graphite, which have indefinitely extended structures, fullerenes have an exact molecular weight and behave as a molecule.

These characteristics allow fullerenes to be solubilized in organic solvents and, therefore, to be chemically modified, obtaining many derivatives that, in general, preserve the exceptional physicochemical properties of their precursors [1–3].

Fullerenes behave like poly-olefins that are deficient in electrons; thus, they share the typical reactivity of these type of molecules. Several synthetic strategies were developed to functionalize this class of compounds, including Diels-Alder cycloaddition [4], Bingel-Hirsh cyclopropanation [5], and 1,3-dipolar cycloaddition of azomethine ylides via the Prato reaction [6], [7]. Among all of the previously mentioned methodologies, the Bingel reaction has undoubtedly been one of the most employed approaches to obtain various fullerenes derivatives. This reaction consists of a cyclopropanation that is catalyzed by a strong base, usually sodium hydride (NaH) or 1,8-diazabicyclo (5.4.0) undec-7-ene (DBU), to introduce α-haloester or α-haloketone ligands to two fullerene carbon atoms [8,9].

This reaction occurs through an addition-elimination mechanism. The first step involves the formation of a carbanion by the deprotonation of the active methylene group, which is then added to one of the sp^2 carbons of the double bond. This cyclopropanation process was also carried out with malonates in the presence of I_2 or CBr_4 and a base, generating *in situ* α-halomalonate and, subsequently, the respective fullerene derivatives [10,11].

As mentioned above, fullerene derivatives, especially those of C_{60} and C_{70}, have unique physicochemical properties; for this reason, they have been largely investigated for their potential application in a broad variety of technological areas. Fullerenes have been successfully employed in the development of solar cells [12,13] in the medical field [14] as photodynamic therapy sensors [15], as molecularly photoactive devices [16], as magnetic and catalytic materials [17], and as bacterial growth inhibitors [18]. Fullerenes have played an important role in the field of solar cells as their spherical shape generates a system of delocalized π electrons that allows them to behave as good electron acceptors. Additionally, they have a low reduction potential [19].

The modification of perovskite-type solar cells using C_{60} and C_{70} derivatives has generated a lot of interest since these structures stand out from other materials thanks to their interesting characteristics such as high absorption coefficients, simple structures, low process temperatures, and lack of complications due to hysteresis. In terms of the application of symmetrically substituted cyclopropanefullerenes in the design of solar devices, Troshin *et al*. [20] previously showed that the presence of different substituents in the cyclopropane ring could enhance the energy output parameters of photovoltaic devices. A representative example of this application was the work published by Echegoyen *et al*. [21] in 2016, in which this type of solar cell was modified with the derivatives 2,5-(dimethylester)-C_{60}, fulleropyrrolidine ($DMEC_{60}$), and its analogue with C_{70} ($DMEC_{70}$) to reach PCE of 15.2% and 16.4%, respectively. In 2017, Echegoyen *et al*. [22] modified these materials using a dimer derivative of C_{60} (D-C_{60}) formed from two units of the [6,6]-phenyl-C_{61}-butyric acid methyl ester ($PC_{61}BM$). By doing this, they obtained a cell with the ability to efficiently passivate the energy states between the layers of fullerene and perovskite, which leads to better electron extraction and a photovoltaic performance of 16.6%. Recently, Ye *et al*. [23] made modifications to the perovskite solar cells (PSCs) by adding the bis(1-[3-(methoxycarbonyl)-propyl]-1-phenyl)-[6,6]C_{62}(bis-PCBM) doped with decamethylcobalt (DMC), which generated a device with both good stability and an efficiency of 20.14%.

This investigation focuses on the synthesis, characterization, and study of the photovoltaic properties of the diacetylmethane monoadducts of C_{60} and C_{70}. These derivatives were obtained from a Bingel reaction, and each of the respective fullerenes, carbon tetrabromide, and DBU in *ortho*-dichlorobenzene (*o*-DCB) were adopted as shown in Figure 1. This

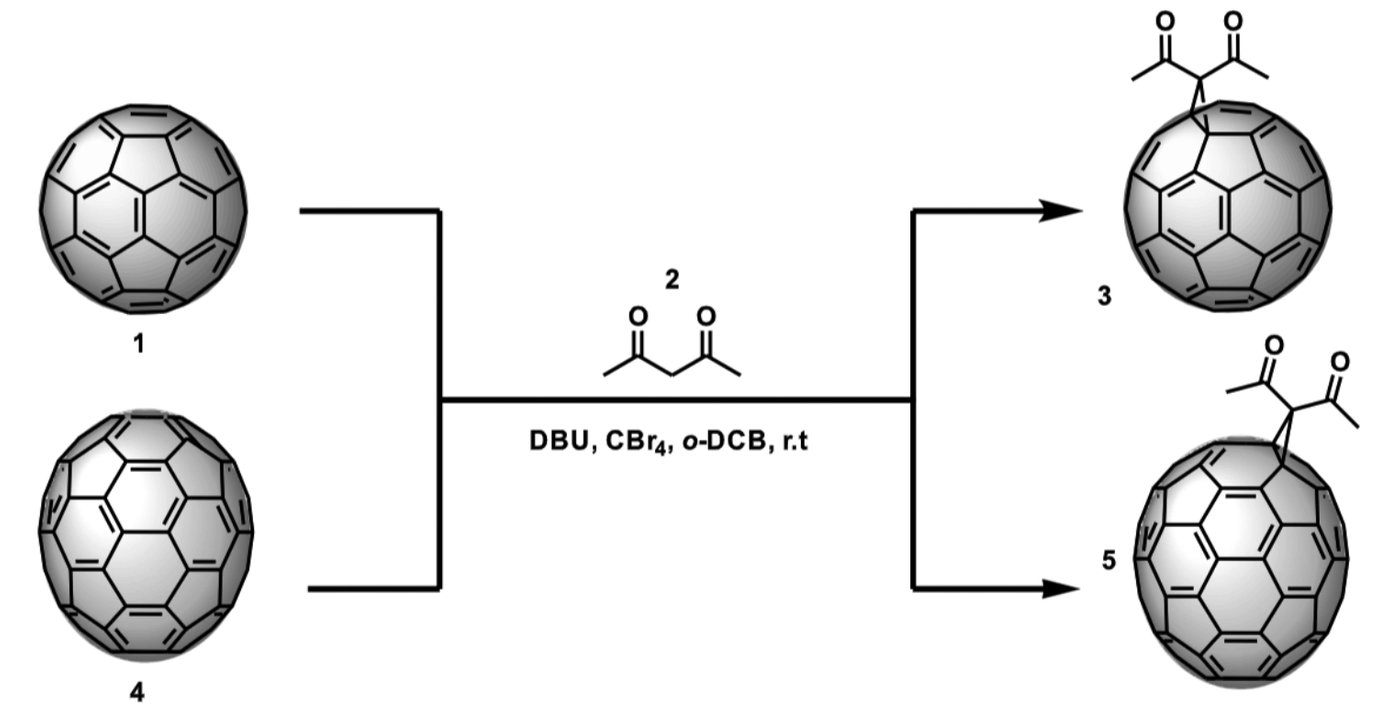

Figure 1. Synthesis of the C_{60} and C_{70} fullerene diacetylmethane monoadducts.

exo-functionalization was carried out to generate a greater structural diversity on C_{60} and C_{70} fullerenes and, consequently, to synthetize compounds that can increase the efficiency of energy conversion in perovskite-type solar cells. These compounds have a straightforward, non-expensive synthesis and are easily purified.

Materials and methods

Reagents

(C_{60}-I_h) [5,6] fullerene, (C_{70}-D_{5h}) [5,6] fullerene, 1,8-Diazabicyclo [5.4.0] undec-7-ene (DBU), and carbon tetrabromide (CBr_4) were purchased from Sigma Aldrich® (USA); they were used without prior purification. Chloroform ($CHCl_3$), carbon disulfide (CS_2), *o*-dichlorobenzene (*o*-DCB, $C_6H_5Cl_2$), and hexane (C_6H_{14}) of analytical grade and silica gel (63-200 Mesh) were purchased from Panreac®. Acetylacetone (acac, $C_5H_8O_2$) was purchased from Alfa Aesar®, and chloroform-d_1 ($CDCl_3$) was purchased from Merck®(EE. UU.). The reagents were analytical grade. The TLC conditions were: silica-gel 60 F_{254} layers with fluorescence indicator.

Instruments

IR spectra of the products were recorded with a Shimadzu® (Japan) IR prestige-21 spectrophotometer in ATR mode. The spectra were processed with the IR_solution® software.

UV-Vis spectra were recorded on a ThermoScientific® (United Kingdom) Evolution-300 spectrophotometer by dissolving a sample of the solid product (ca. 5 mg) in chloroform. The spectra were recorded between 250 and 750 nm wavelength (λ) using a quartz cell (optical path of 1 cm). The spectra were processed using the VisionPro® software.

^{1}H and ^{13}C NMR spectra were recorded on a Bruker® (Germany) 400 MHz spectrometer, using chloroform-d_1 ($CDCl_3$) as the solvent and internal standard. The spectra were processed with the MestReNova® software.

Cyclic Voltammetry (CV) and Osteryoung Square Wave Voltammetry (OSWV) were conducted in *o*-DCB with NBu_4PF_6 as the supporting electrolyte and using a 1-mm-diameter glassy carbon disk as the working electrode. Ferrocene was added at the end of the experiments to be used as internal reference to measure the potentials.

Matrix-assisted laser desorption/ionization – time of flight - mass spectrometry (MALDI-TOF-MS) was carried on positive mode, with samples dissolved in chloroform and using 1,1,4,4-tetraphenyl-1,3-butadiene (TPB) as the matrix.

Current-Voltage (*J-V*) performance of the devices was tested using a Keithley 2420 source meter under a Photo Emission Tech SS100 Solar Simulator. The light intensity was calibrated using a single-crystal Si photovoltaic cell as the reference. The measurements were made in air at room temperature.

General methodology for the C_{60} and C_{70} cyclopropanation reaction

The C_{60}/C_{70} fullerene (1 mmol) was dissolved in 5 mL *o*-dichlorobenzene (*o*-DCB) in a 25 mL round bottom flask. Then, the acetylacetone (0.5 mmol) and CBr_4 (0.5 mmol) were added to this solution. Subsequently, the DBU (0.5 mmol), previously dissolved in 3 mL of the *o*-DCB, was added drop-by-drop at room temperature to the reaction mixture under stirring. The total time of the reaction was one hour. Once the reaction was finished (TLC check adopting CS_2 and $CHCl_3$ as the mobile phase, silica-gel 60 F_{254} layers with fluorescence indicator, room temperature), the crude reaction product was purified by column chromatography on silica gel (17 g), using hexane, carbon disulfide, and chloroform as eluents. The chromatographic separation for both C_{60} and C_{70} derivatives was carried out by first using hexane to extract the *o*-DCB, then carbon disulfide to separate the unreacted precursor, and finally chloroform to obtain the monoadduct of interest.

Synthesis of (C_{60}-I_h)[5,6]fullerene diacetylmethane monoadduct, (3), $C_{65}O_2H_6$

By employing 100 mg (0.14 mmol) of C_{60}, 7.23 µL (0.07 mmol) of acetylacetone, 23.21 mg (0.07 mmol) of CBr_4 and 10.47 µL (0.07 mmol) of DBU, 39.5 mg (0.04 mmol, 69%) of the monoadduct was obtained **(3)**, $C_{65}H_6O_2$ (818.65 g/mol) as a brown solid. Rf: 0.62, IR(ATR): ν (cm^{-1}): 2920, 2849, 1708, 1646, 1461, 1427; ^{1}H-NMR (400 MHz, CS_2/$CDCl_3$): δ (ppm) 2.84 (s,6 H); ^{13}C-NMR (100 MHz, CS_2/$CDCl_3$): δ (ppm) 193.44, 144.53, 145.25, 145.10, 144.80, 144.76, 144.61, 143.79, 143.22, 143.11, 142.32, 142.04, 141.26, 137.77, 74.10, 70.37, 28.12; UV-Vis ($CHCl_3$) λ (nm): 680, 425, 488. Expected exact mass: 818.7, experimental *m/z*: 818.1.

Synthesis of (C_{70}-D_{5h})[5,6]fullerene diacetylmethane monoadduct, (5), $C_{75}O_2H_6$

By employing 100 mg (0.12 mmol) of C_{70}, 6.2 µL (0.06 mmol) of acetylacetone, 19.89 mg (0.06 mmol) of CBr_4, and 8.97 µL (0.06 mmol) of DBU, 25 mg (0.02 mmol, 44%) of the monoadduct was obtained **(5)**, $C_{75}H_6O_2$ (938.75 g/mol), as a black solid. Rf: 0.56, IR(ATR): ν (cm^{-1}) 2917, 2847, 2156, 1707, 1645, 1515; ^{1}H-NMR (400 MHz, CS_2/$CDCl_3$): δ (ppm) 2.80 (s, 6 H); ^{13}C-NMR (100 MHz, CS_2/$CDCl_3$): δ (ppm) 194.59, 155.33, 151.78, 151.15, 150.79, 150.55, 149.39, 149.20, 149.14, 148.53 (2C), 148.51, 148.48, 147.49, 147.35, 146.96, 146.38, 145.94, 145.83, 144.77, 143.99, 143.78, 143.58, 142.78, 141.46, 141.03, 139.71, 136.40, 133.74, 132.86, 130.88, 130.78, 68.24, 67.30, 29.72; UV-Vis ($CHCl_3$) λ/nm: 463, 402, 370, 355. Expected mass: 938.8, experimental *m/z*: 938.1.

Results and discussion

Monoadducts **(3)** and **(5)** were synthesized using Bingel cyclopropanation reaction by combining the selected fullerenes (C_{60} and C_{70}) with acetylacetone in the presence of CBr_4, DBU, and *o*-DCB as solvent, see Figure 1; *o*-DCB was chosen as solvent because of the solubility of the precursors in it (C_{60} 27 mg/mL, 36.2 mg/mL C_{70}) [24,25]. The reaction firstly involves the formation of the α-bromoacetylacetone; then it is followed by an *in situ* cyclopropanation, catalyzed by DBU base, and the product of interest is obtained. DBU is a strong heterocyclic base that reacts rapidly; thus, its addition to the reaction mixture needs to be controlled and slowed to avoid the formation of poly-adducts. The adducts are slightly soluble in chloroform, so it is necessary to add carbon disulfide to have a better result during spectroscopic analysis.

Synthesis of C_{60} fullerene diacetylmethane monoadduct

At the beginning of the synthesis of derivative (3) the C_{60} solution appears violet, but after the addition of DBU the color quickly assumes a wine-red tonality, indicating that a chemical transformation occurred. Employing these working conditions, the product obtained appears to be a brown

solid with a 68% yield (42% considering the recovered precursor). It is interesting to note that the TLC (check adopting CS_2 and $CHCl_3$ as mobile phase on silica) performed as a control during the synthesis showed the formation of the product of interest (3) and as well the formation of other co-products of greater polarity, which, possibly, correspond to poly-adducts generated within the reaction medium. However, these poly-adducts are practically impossible to avoid, because the presence of 30 double bonds [6,6] in C_{60} make it difficult to solely obtain the regiospecific derivatives.

It is important to highlight that only two previous works related to the synthesis of this derivative have been reported in the literature. The first is the work done in 1998 by Bingel who obtained this compound from the reaction of acetylacetone in the presence of iodine, DBU, and toluene with a lower yield of 18%, possibly due the poor solubility of C_{60} in this solvent [26]. The second work, previously cited, was published by Jin *et al*. and describes the synthesis of this monoadduct starting from α-bromoacetylacetone in the presence of DMSO as solvent and Na_2CO_3 as base to form the derivative (3) with a yield of 34% [8]. Based on the results obtained from previous published research as well as this research, it can be deduced that, by controlling the stoichiometry, DBU concentration and the reaction time, the derivative (3) can be formed with a good yield.

After having separated and purified the products by column chromatography on silica gel, the structural characterization of the product (3) was carried out by UV-Vis, infrared, nuclear magnetic resonance (^1H and ^{13}C) spectroscopy, and mass spectrometry (MALDI).

The UV-Vis spectrum gave the first indication that the formation of C_{60} monoadduct (3) took place because of the appearance of the absorption bands at 425 nm (Figure 2) that show a behavior similar to the characteristics of a C_{60} monoadduct spectrum [27]. The absorption band at 324 nm was interpreted as an electronic transition from the pi-bonding orbital to the pi-antibonding orbital ($\pi - \pi^*$) of the fullerene unit. Additionally, it is blue-shifted with respect to the C_{60} band due to the disruption of the sp^2 conjugation when the [6,6] double bond is removed. In toluene, there is a bathochromic shift of about 4.0 nm, which can be correlated to the solvation processes [28].

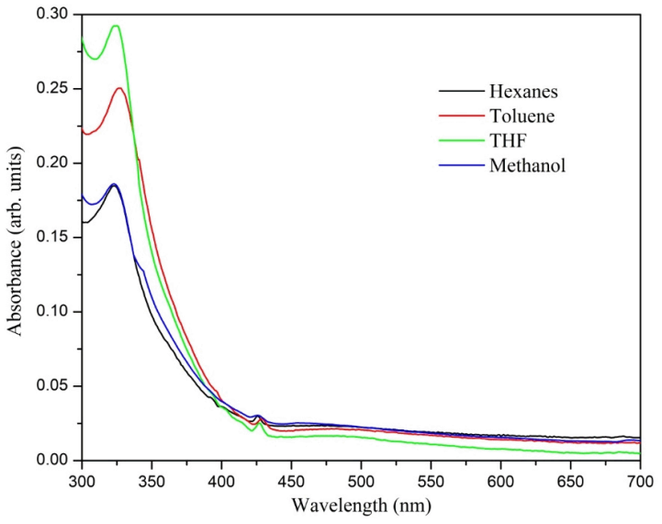

Figure 2. UV-Vis absorption spectra recorded of the compound (3) C_{60} monoadduct in different solvents.

A secondary indication that confirms the preliminary formation of (3) was found in the infrared spectrum (Figure 3), where the stretching of the sp^3 hybridized C-H bond in the methyl group can be observed in the bands at 2920 and 2849 cm^{-1}. Additionally, the absorption bands associated with the out-of-plane and in-plane bending vibrations of the methyl group are observed at 1356 and 1426 cm^{-1}, respectively. Moreover, the absorption band of the C=O stretch was found at 1708 cm^{-1}, while the C=C bond stretch was recorded at 1646 cm^{-1}.

The identity of product (3) was confirmed with the information provided by the nuclear magnetic resonance spectrum. ^1H spectrum (Figure 4 a) showed a singlet at 2.84 ppm generated by the methyl protons of the carbon directly bonded to the carbonyl. The ^{13}C spectrum (Figure 4 b) also showed the expected signals. Cycloaddition of a symmetric fragment along the 6,6 bond results in a ^{13}C-NMR spectrum of such a cycloadduct containing 17 peaks of fullerene carbon atoms. Among these, it was possible to observe that σ 70–90 ppm is typical for sp^3 hybridized atoms, and the other 16 localized between 137 and 160 ppm are characteristic of the sp^2 fullerene carbon atoms.

Specifically, the signals at 28.12 and 70.37 ppm are characteristic of the sp^3 carbons belonging to the methyl group and the quaternary carbon present from the adduct, respectively, while the signal at 74.10 ppm is due to carbons 1 and 2 from the cage. The signal observed at 193.44 ppm, close to the intense CS_2 solvent pick, is due to the carbonyl group, and only 13 of the 17 signals expected for the cage (C3-60) are observed since some signals overlap. All signals confirm a C_{2v} symmetry for the monoadduct, as expected [9]. These results agree with those reported by Bingel [26].

Synthesis of C_{70} fullerene diacetylmethane monoadduct

A color change occurred during the reaction; in fact, the crude mixture turned from red to dark brown. This indicated that a chemical transformation was taking place. The reaction was followed-up by TLC, where the expected monoadduct product appeared, eluting below the precursor. Similarly to the synthesis of (3), other products, which correspond to poly-adducts formed as a consequence of the multiple reactive bonds present in fullerenes were eluted below (5) in the chromatographic column.

It is important to highlight that C_{70} has four types of [6,6] bonds, referred to as γ, δ, α, and β [27,29]. These last two bonds, in particular, prove to be the most reactive in this molecule, and that is why this reaction can generate both the α and β isomer. However, the literature reports that the Bingel reaction generates a product with high regioselectivity on the C_{70}. This is a consequence of the nucleophilic attack on the α-bond close to the polar zone of the fullerene [30] where the pyramidalization (the distortion from the plane geometry to a pseudo-tetrahedral symmetry) of the sp^2 hybridized carbon atoms and the angle of curvature of the fullerene decreases moving from the poles to the equator, and, therefore, the attack on a α-bond becomes the most feasible for a transannular structure, such as the one formed during the Bingel reaction. The reason why this can be assumed with good probability is that the product obtained under these reaction conditions was the α isomer [31,32]. This behavior was also reported with hydroalkylations, hydroarylations, Diels-Alder reaction, and dipolar cycloadditions [3+2] of nitrile oxides in C_{70}. It is worth mentioning that the 1,3-dipolar cycloaddition of azomethine ylides is the least regioselective reaction on C_{70} since it leads to the α, β, and γ isomers in different proportions, depending on the reaction conditions and the nature of the azomethine ilyde [32,33]. It is important to mention that we did not find the β isomer while carrying out column chromatography and purification, and we also did not find it in NMR spectra.

The UV-Vis spectrum (Figure 5) shows four absorption bands recorded at 461, 405, 371, and 352 nm, which appear similar to those reported in the literature for a Bingel monoadduct substituted in the α position of the C_{70} [34,35]. This suggests that the compound of interest was formed. Similar to (3), each absorption band recorded in the spectrum was associated with possible electronic transitions: The transitions of the carbonyl group from the non-bonding orbital to the pi-antibonding (n-π^*) at 461 nm, from the pi-bonding to pi-antibonding ($\pi - \pi^*$) at 405 nm, and the transitions of the fullerene double bonds from the pi-bonding to pi-antibonding orbital ($\pi - \pi^*$) at 371 and 352 nm. The intensity of the absorption bands decreases as the polarity of the solvent increases, and this can be attributed to the stability of the charge-transfer states in the C_{70} monoadduct, which is more

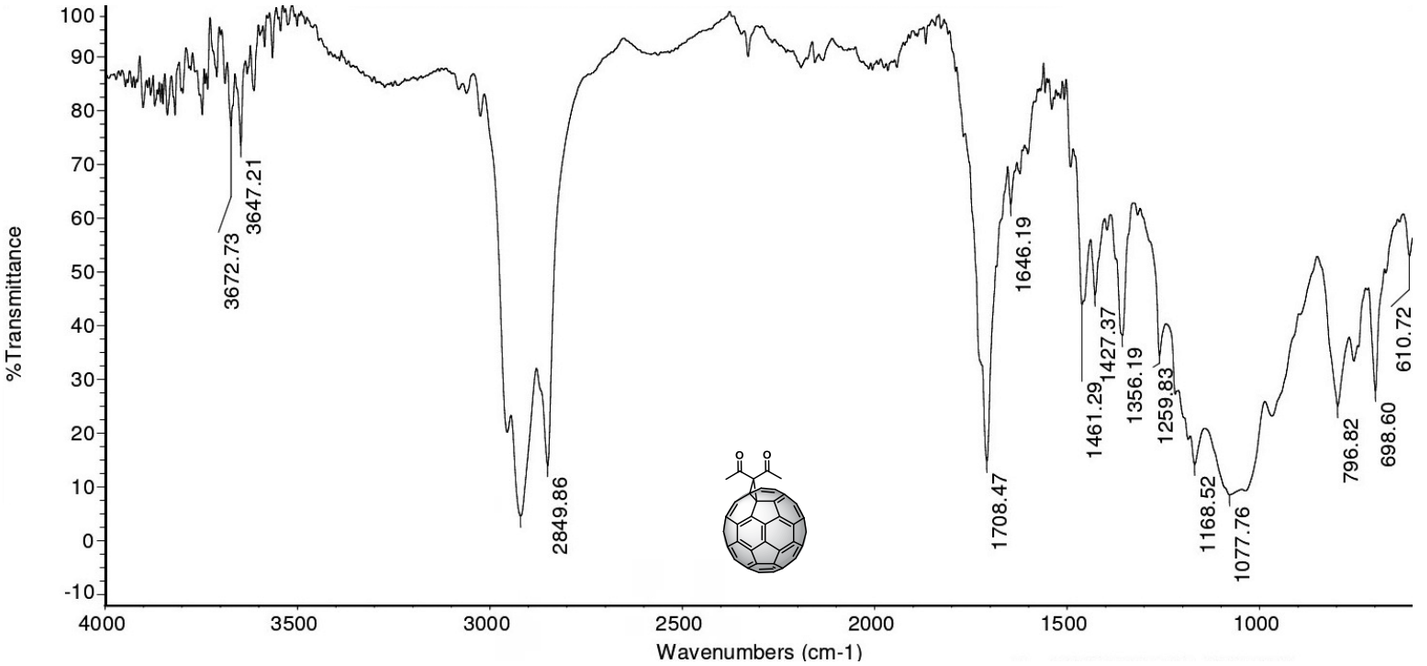

Figure 3. IR spectrum in ATR mode of compound (3) C_{60} monoadduct.

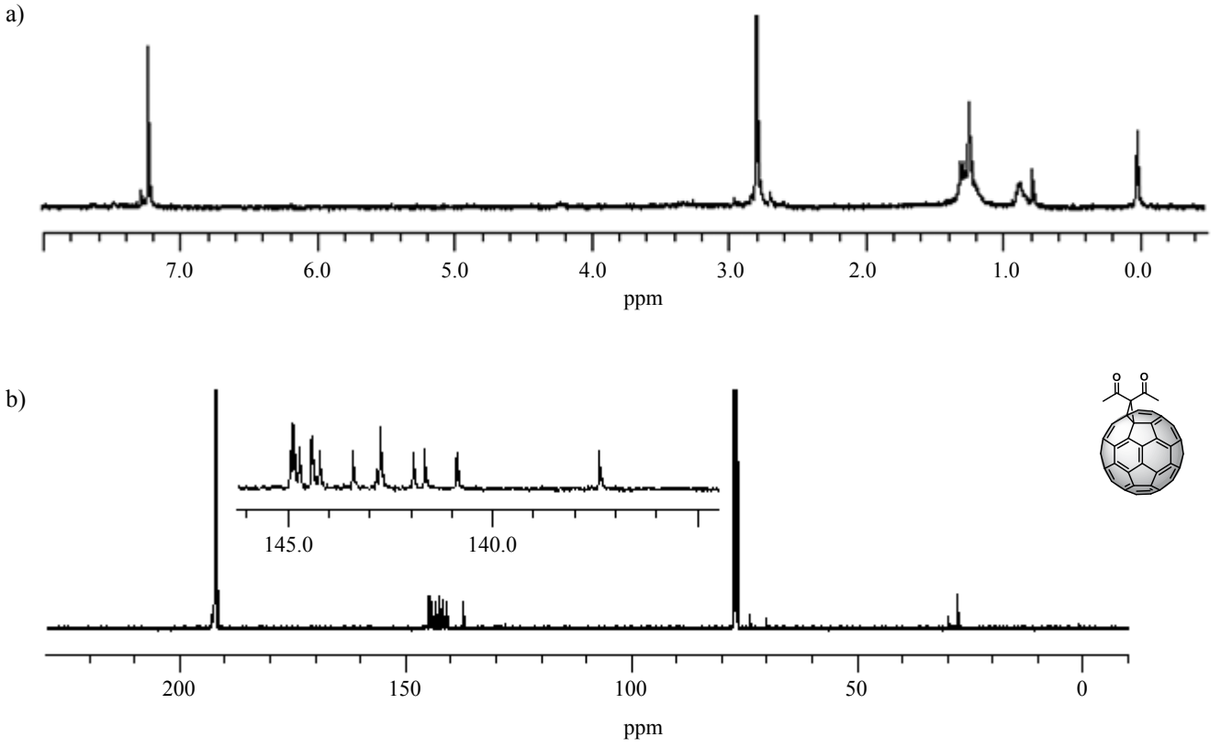

Figure 4. a) ^{1}H-NMR spectrum (CS_2/$CDCl_3$, 60 MHz) and **b)** ^{13}C-NMR spectrum (CS_2/$CDCl_3$, 100 MHz) of compound (3) C_{60} monoadduct. H signals of the monoadduct are singlets. C insets are amplifications of the cage's chemical shift zone.

stable in polar solvents, such as methanol [36]. In the same way as the C_{60} monoadduct, the C_{70} presented a brief solvatochromic effect of about 4 nm in toluene, possibly due to the solvation.

An IR spectrum analysis allows an initial raw characterization of the product from the cyclopropanation (5). The spectrum (Figure 6) shows the vibration bands corresponding to the symmetric and asymmetric stretching and out-of-plane and in-plane bending of the methyl group in the

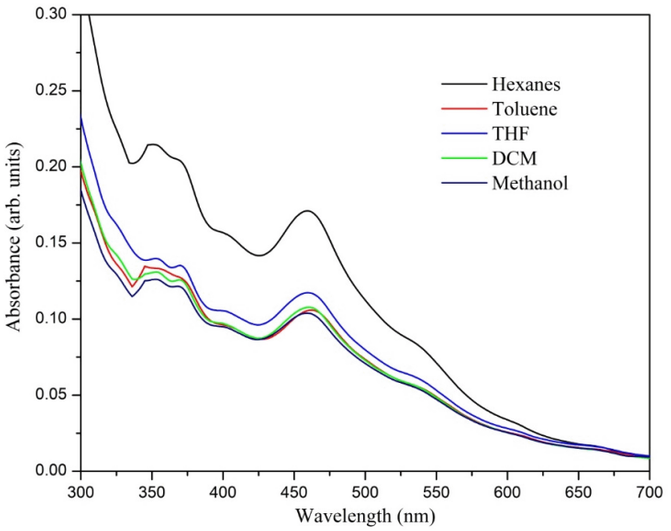

Figure 5. UV-Vis absorption spectra of the compound (5) C_{70} monoadduct, recorded in different solvents.

following regions: 2916 - 2848 cm^{-1}, 1353 cm^{-1}, and 1426 cm^{-1}, respectively. The presence of the carbonyl group is confirmed by the presence of the intense absorption band at 1707 cm^{-1}, caused by the stretching of the C=O bond. The presence of the C=C bond is confirmed by the absorption band at 1645 cm^{-1}, which is caused by its stretching vibration.

The ^{1}H NMR spectrum (Figure 7 a) provided valuable information that confirmed the formation of the product of interest, since the singlet registered at 2.80 ppm corresponds to the six symmetrical methyl protons present in (5). Like the spectrum of the C_{60} monoadduct, there are other signals that do not belong to the C_{70} monoadduct that are due to impurities present in the sample, which register between 0.88-1.44 ppm, and could possibly be from grease present in the materials employed. The ^{13}C NMR spectrum (Figure 7 b) reports the expected signals. In particular, the carbons of the methyl group appear at 29.72 ppm, the ring carbon (sp^3-C) at 67.30 ppm, and the carbons 1 and 2 of the cage at 68.24 ppm. The signal of the carbonyl group can be observed at 194.59 ppm, and for the 34 expected signals of the sp^2 hybridized carbons from the fullerene cage (C3-60), only 31 signals are observed in the range 130.74 to 155.33 ppm due to peak overlapping. All the signals confirmed the presence of the expected C_1 symmetry for the monoadduct. These results agree with those previously published by Bingel and Hermann *et al.* [34] and, as previously mentioned, the product obtained appears to be the α derivative due to the bond's very high reactivity [37,38] The formation of other monoadducts was not detected, and, according to the current knowledge, there are no previous reports of the C_{70} diacetylmethane monoadduct.

Electrochemistry

Previous studies reported that Bingel derivatives of C_{60} and C_{70} exhibit quasi and reversible cathodic electrochemical behavior [39–41] CV of C_{60}-diacetylmethane (3) and C_{70}-diacetylmethane (5) compounds were recorded at a scan rate of 100 mV/s (Table 1 and Figure 8). Compound (3) exhibits seven irreversible reduction peaks in which four are well-defined. Based on their shape and current intensity, these are likely to be monoelectronic. On the other hand, compound (5) exhibits six reduction events. Four of these were well-defined, and as with compound (3), all the peaks are irreversible and monoelectronic. No oxidation events were observed for either compound—at least none within the work potential window.

Table 1. Redox potential peaks of fullerene acetylacetone monoadducts.

Compound	E^1_{pc}/V	E^1_{pa}/V	E^2_{pc}/V	E^2_{pa}/V	E^3_{pc}/V	E^3_{pa}/V
3	-1.52	-0.95	-1.85	-1.46	-2.05	-1.76
5	-1.36	-0.90	-1.71	-1.43	-2.10	-1.83

Figure 9 shows the cyclic voltammogram for the first reduction potential of compound (3) (left figure) and its behavior as the scan rate is increased from

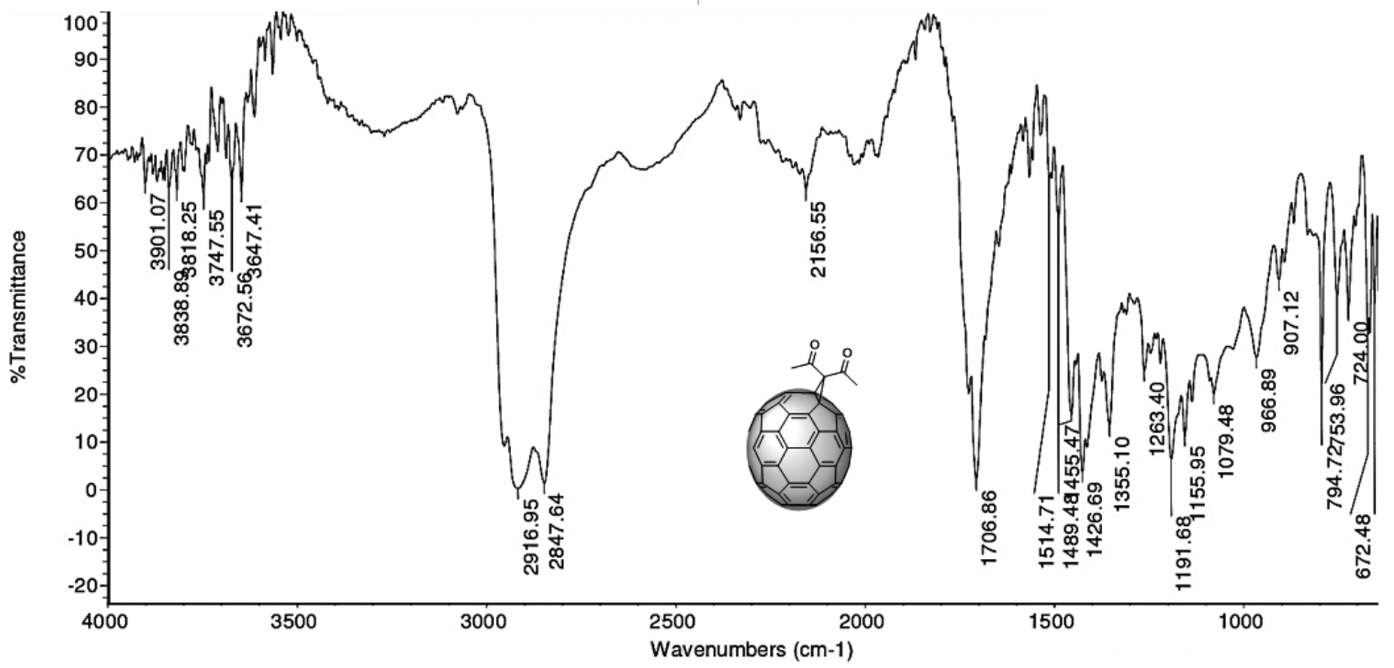

Figure 6. IR spectrum in ATR mode of compound (5) C_{70} monoadduct.

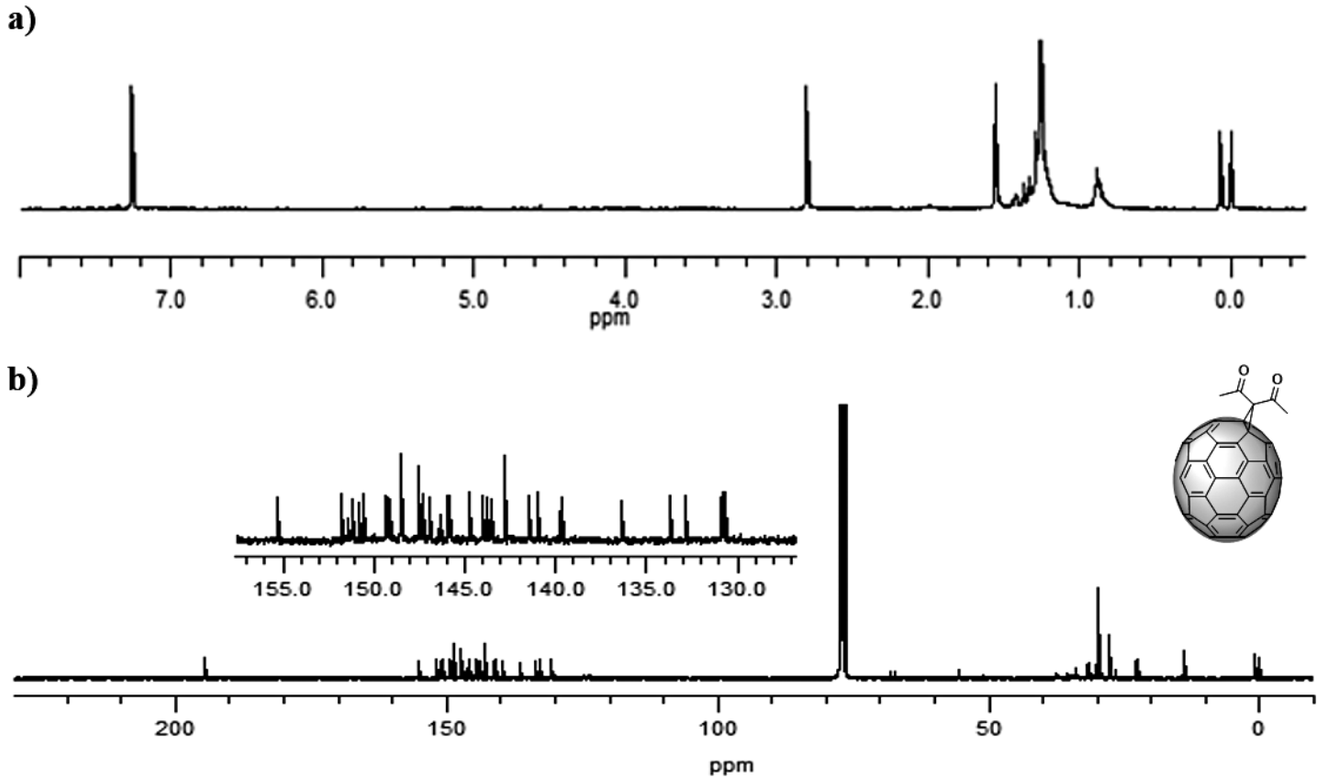

Figure 7. a) ^{1}H-NMR spectrum ($CS_2/CDCl_3$, 60 MHz) and **b)** ^{13}C-NMR spectrum ($CS_2/CDCl_3$, 100 MHz) of compound (5) C_{70} monoadduct. H signals of the monoadduct are singlets. C insets are amplifications of the cage's chemical shift zone.

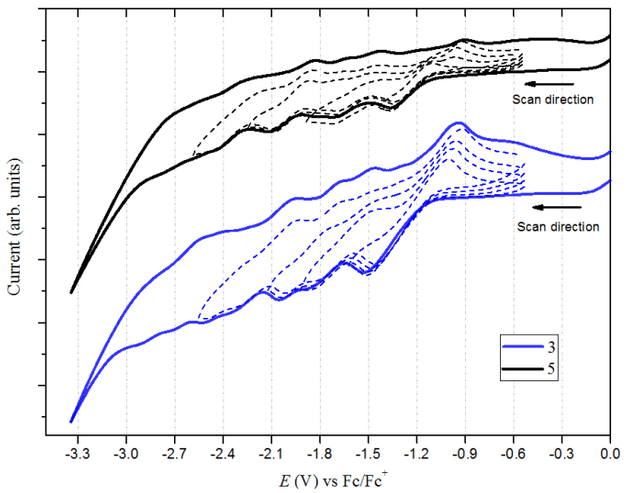

Figure 8. Cyclic voltammetry (0.05M $TBAPF_6$/*o*-DCB, 100 mV/s scan rate) of compound **(3)** C_{60} monoadduct and compound **(5)** C_{70} monoadduct. Dotted lines are the individual scans for each peak potential.

100 to 500 mV/s. The current intensity is increased, and the potential is shifted as the scan rate goes higher, which is a typical characteristic of irreversible processes. This behavior was also observed for compound (5) (right figure). Furthermore, there is a linear dependence between the peak current and the square root of the scan rate, a fact that confirms that the electron transfer is regulated by diffusion. With this knowledge, it is possible to calculate the diffusion coefficients through the Randless-Sevcik equation (see Figure 10 and Table 2).

Table 2. Diffusion coefficients for each reduction potential of fullerene acetylacetone monoadducts.

Compound	(3)			(5)		
	E^1_{red}/V	E^2_{red}/V	E^3_{red}/V	E^1_{red}/V	E^2_{red}/V	E^3_{red}/V
***D*/cm^{2}min^{-1}**	0.42	0.60	1.39	0.11	0.48	0.55
R^2	0.9529	0.9984	0.9857	0.9688	0.9942	0.9871

* The molar concentration of each solution was $4.3x10^{-6}$ mol/mL.

Furthermore, Osteryoung Square Wave Voltammetry (OSWV) was carried out for compounds (3) and (5). For both compounds, six reduction waves were observed (Table 3 and Figure 11). Both fullerene derivatives exhibit a cathodic shift in the first reduction potential, compared to the pristine C_{60} fullerene and C_{70} fullerene. Based on the first reduction potential, the LUMO energy level was calculated to be -3.09 and -3.13 eV for (3) and (5), respectively. Comparing these values with $PC_{61}BM$ (-3.90 eV) and other Bingel fullerene derivatives, the compounds of this study are also higher than the LUMO energy of the traditional perovskite $MAPbI_3$, which allows the conductance of the electron flux.

It is possible to replace C_{60} with C_{70} in derivatives for the electron transport layer (ETL) and develop highly efficient solar cells [44]. The loss of symmetry in the fullerene C_{70} makes fewer forbidden transitions, representing a higher probability for HOMO-LUMO transitions [45]. As we can see in the UV spectra (Figure 2 and Figure 5) and the cyclic voltammetry (Figure 9), the differences in the spectral range of absorption between both derivatives allows us to conclude the highest efficiency value is expected for compound **(5)**. As expected, there is a significantly stronger absorption in the visible region, and an increase in the external quantum efficiency for C_{70} adducts.

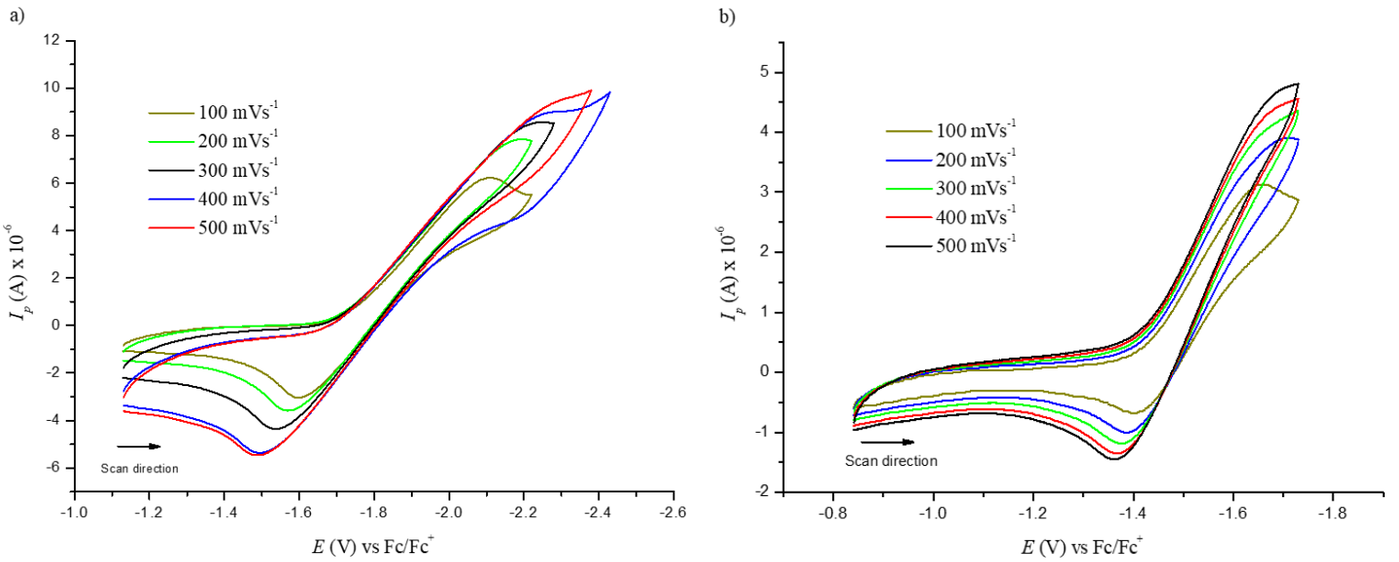

Figure 9. Cyclic voltammetry of the first peak reduction at different scan rates for a) compound (3) C_{60} monoadduct and b) compound (5) C_{70} monoadduct.

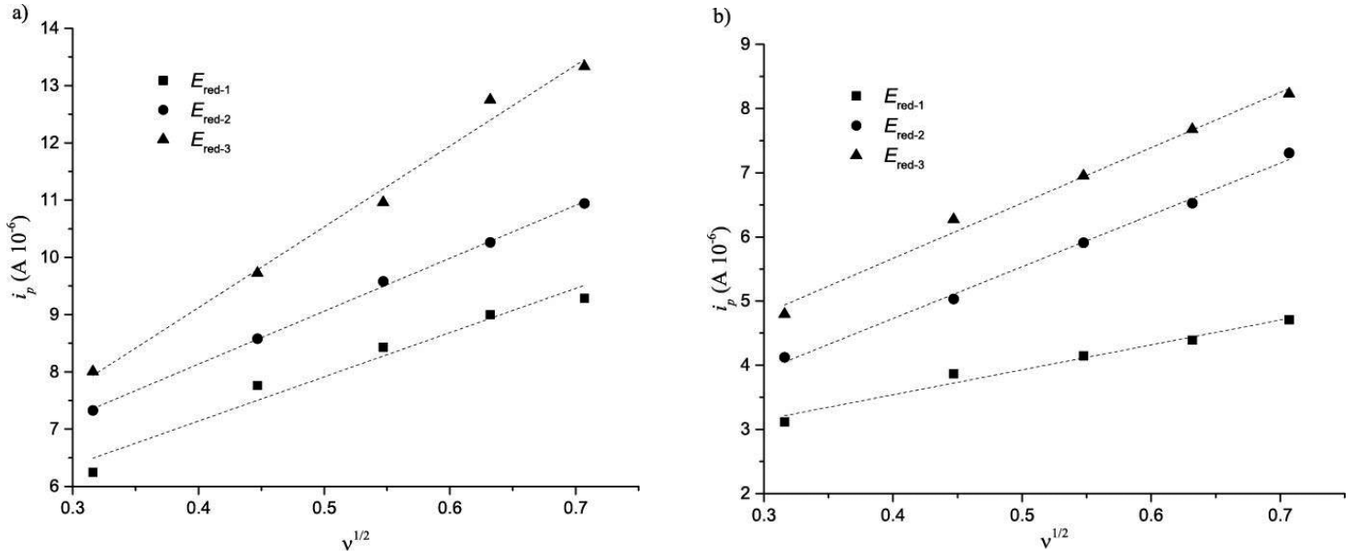

Figure 10. Dependence of the current peak with the square of the scan rate for each reduction potential of **a)** compound (3) C_{60} monoadduct and **b)** compound (5) C_{70} monoadduct.

Table 3. Comparison of the potential reduction values of fullerene acetylacetone monoadducts and pristine fullerenes.

Compound	E^1_{red}/V	E^2_{red}/V	E^3_{red}/V	E^4_{red}/V	E^5_{red}/V	E^6_{red}/V	LUMO[c] (eV)
C_{60}[a]	-1.00	-1.40	-	-1.86	-2.31	-	-3.72
3	-1.63	-1.91	-2.13	-2.41	-2.55	-2.74	-3.09
C_{70}[b]	-1.07	-1.39	-	-1.90	-2.36	-	-3.65
5	-1.59	-1.91	-2.02	-2.32	-2.63	-2.70	-3.13

[a] From the reference[42] [b] From the reference[43] [c] From the equation LUMO = -(4.72 + E_{red}^{on}).

According to Dai and co-workers, the different molecular aggregation can explain the results of a better ETL by using a formulation with a mixture of the $PC_{71}BM$ isomers instead the isolated isomers [46]. This fact, and the higher solubility of C_{70} compounds compared to C_{60} ones, reduce the disorder in the ETL, increasing the quasi-Fermi level of the photogenerated electrons and also reducing the pinholes as well [47]. This aspect can be confirmed with the higher value of V_{oc} and may also elucidate the different values of PCEs in this work.

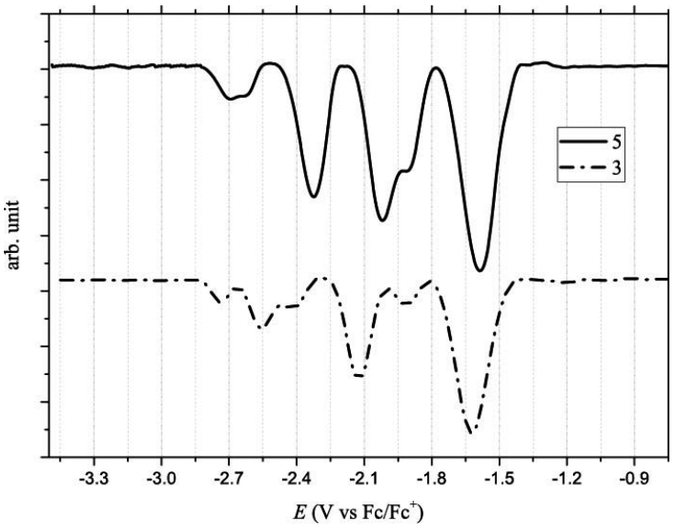

Figure 11. Osteryoung Square Wave Voltammetry in 0.05M $TBAPF_6$/*o*-DCB of compound **(3)** C_{60} monoadduct and compound **(5)** C_{70} monoadduct.

Photovoltaic Performance

The results from the electrochemistry combined with the UV-Vis characteristics allowed us to obtain the work function for the compounds (3) and (5), which is vital information to determine whether they are suitable or not to be used as an ETL in PSCs. HOMO and LUMO values of compounds (3) and (5) are summarized in Table 4. Figure 12 shows that HOMO-LUMO values of the compounds (3) and (5) do not match very well with those of the perovskite layer, which can lead to an inefficient hole blocking process and hysteresis behavior in the PSCs. This phenomenon makes part of the experimental work in the understanding of charge generation at organic heterojunctions and charge separation. High-level theoretical calculations as semiempirical and density functional molecular calculations could be carried out in order to understand the dynamics of charge pair generation and correlate the theoretical LUMOs with the open circuit voltage of the photovoltaic device [48,49].

Table 4. Photovoltaic performance of the control $PC_{61}BM$, of compound **(3)** C_{60} monoadduct and compound **(5)** C_{70} monoadduct.

Compound	λ_{abs} (nm)	E_g (eV)	LUMO (eV)	HOMO (eV)
$PC_{61}BM$	718	1.73	-3.99	-5.65
3	713	1.74	-3.09	-4.83
5	710	1.75	-3.13	-4.88

Device fabrication

The device fabrication followed the procedure adopted by Fernández-Delgado *et al*. [50] who probed the variation of interfacial interactions of $PC_{61}BM$-like electron transporting compounds for PSC.

PSCs with an ITO/NiO_x/$CH_3NH_3PbI_3$/ETL/Ag configuration were fabricated (Figure 12) to study the capacity of the compounds (3) and (5) to act as ETLs. Chlorobenzene was employed as a solvent for the deposition of adducts (3) and (5).

The *J-V* curves for the fabricated PSCs are shown in Figure 13. $PC_{61}BM$ as ETL was used as the control and revealed an average PCE value of 14.9%, an open circuit voltage (V_{oc}) of 1.01 V, a fill factor (FF) of 64%, and

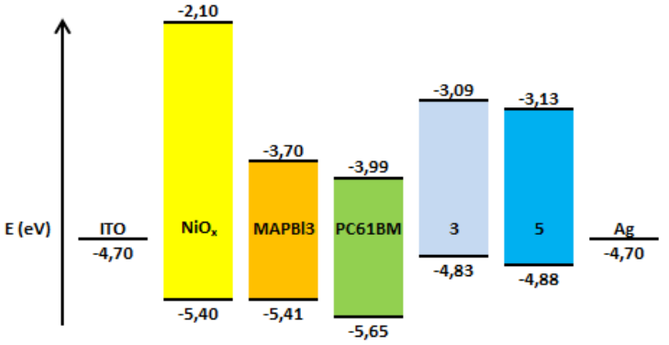

Figure 12. Energy levels for the different layers of the PSCs.

a short circuit current (J_{sc}) of 23.0 mA/cm^2. The PSCs performances are summarized in Table 5.

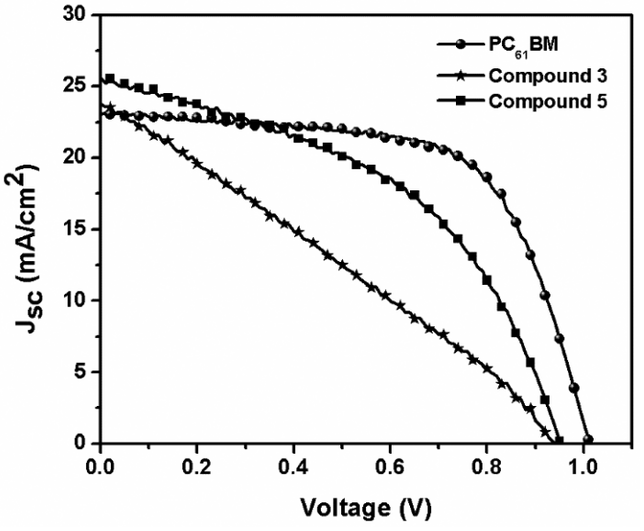

Figure 13. control $PC_{61}BM$, compound **(3)** C_{60} monoadduct and compound **(5)** C_{70} monoadduct *J-V* curves.

The results show a clear difference between the two fullerene derivatives, with compound (5) showing a better performance with values of PCE very close to that of the control device. As can be distinguished in Figure 13, compound (5), has a better performance, a smaller hysteresis, and a higher current density and voltage value. This behavior can be explained by a better matching of the energy levels to those with the perovskite by an enhanced light absorption of this material and better interface perovskite/fullerene quality, which results in less hysteresis, better FF, and reduced current leakage. All those factors can improve device performances, making this material a suitable ETL in PSCs.

Table 5. Photovoltaic performance of the control $PC_{61}BM$, of compound **(3)** C_{60} monoadduct and compound **(5)** C_{70} monoadduct.

Compound	V_{oc} (V)	J_{sc} (mA/cm^2)	FF	PCE
$PC_{61}BM$	1.01	23.0	0.64	14.9
(3)	0.94	23.8	0.38	8.50
(5)	0.96	25.6	0.57	14.0

Conclusions

By controlling the stoichiometry and the reaction time, and through a knowledge of the mechanistic issues of the fullerene functionalization reactions and their complex molecular geometry that differentiates their reactivity, the synthetic yield of the C_{60} diacetylmethane monoadduct was improved, with respect to what was previously reported in the literature. In addition, the new compound, the C_{70} diacetylmethane monoadduct, was synthesized, and it was obtained with a moderately high yield. The monoadducts were tested in photovoltaic performance studies, and a solar cell efficiency of 8.5 and 14.0 was obtained for compound (3) and (5), respectively. The low values are related to the mismatch in the energy levels of the derivatives when compared to the perovskite, which produces hysteresis and current leakage in the PSCs. Even though the compounds were not very compatible as an ETL, compound (5) exhibited the highest performance, very close to $PC_{61}BM$, which was used as a control. Likewise, OSWV and CV were conducted for compounds (3) and (5), showing irreversible reduction potentials controlled by electron transfer diffusion. Both compounds present LUMOs energy levels higher than the traditional $MAPbI_3$ perovskite one. The optical absorption range and the morphology of ETL may explain a higher value for the C_{70} derivative compared with C_{60} diacetylmethane.

Acknowledgements

The authors would like to acknowledge the unconditional support given by Professor Dr. Luis Echegoyen from the Department of Chemistry and Biochemistry in the University of Texas at El Paso (UTEP), and the kind collaboration of the College of Science at UTEP, Professor Dr. Andrew Evans from Bethel University for his helpful comments and Olivia Fernandez from UTEP for the photovoltaic and MALDI measurements. M.N.C. is deeply grateful to Universidad del Valle for his sabbatical leave.

Funding information

Funding for this research was provided by: Universidad Nacional de Colombia, Facultad de Ciencias (grant No. 45627 to A. Duarte-Ruiz); Departamento Administrativo de Ciencia, Tecnología e Innovación - MINICIENCIAS (grant No. 110171249591 to A. Duarte-Ruiz) and the Vicerrectoría de Investigaciones from the Universidad del Valle (C.I. 71155).

References

[1] S. F. A. Acquah, A. V. Penkova, D. A. Markelov, A. S. Semisalova, B. E. Leonhardt, and J. M. Magi, "Review—the beautiful molecule: 30 years of c60 and its derivatives," *ECS J. Solid State Sci. Technol.*, vol. 6, no. 6, pp. M3155–M3162, 2017. DOI: https://doi.org/10.1149/2.0271706jss.

[2] A. Astefanei, O. Núñez, and M. T. Galceran, "Characterisation and determination of fullerenes: A critical review," *Anal. Chim. Acta*, vol. 882, pp. 1–21, 2015. DOI: https://doi.org/10.1016/j.aca.2015.03.025.

[3] A. Hirsch, *The Chemistry of the Fullerenes*. Stuttgartt: WILEY-VCH, 1994. DOI: https://doi.org/10.1002/9783527619214.

[4] Á. Duarte-ruiz, K. Wurst, and B. Kräutler, "Regioselective one-pot synthesis of antipodal bis-adducts by heating," *Helv. Chim. Acta*, vol. 84, pp. 2167–2177, 2001. DOI: https://doi.org/10.1002/1522-2675(20010815)84:8<2167::AID-HLCA2167>3.0.CO;2-V

[5] C. Bingel, "Cyclopropanierung von fullerenen," *Chem. Ber.*, vol. 126, pp. 1957–1959, 1993. DOI: https://doi.org/10.1002/cber.19931260829.

[6] V. Garg *et al.*, "Conformationally constrained macrocyclic diporphyrin-fullerene artificial photosynthetic reaction center," *J. Am. Chem. Soc.*, vol. 133, no. 9, pp. 2944–2954, 2011. DOI: https://doi.org/10.1002/cber.19931260829.

[7] M. Maggini, G. Scorrano, and M. Prato, "Addition of azomethine ylides to C60: Synthesis, characterization, and functionalization of fullerene pyrrolidines," *J. Am. Chem. Soc.*, vol. 115, no. 21, pp. 9798–9799, 1993. DOI: https://doi.org/10.1021/ja00074a056.

[8] B. Jin *et al.*, "DMSO: An efficient catalyst for the cyclopropanation of C60,C70, SWNTs, and graphene through the bingel reaction," *Ind. Eng. Chem. Res.*, vol. 54, no. 11, pp. 2879–2885, 2015. DOI: https://doi.org/10.1021/ie504918f.

[9] A. Hirsch and M. Brettreich, *Fullerenes: Chemistry and reactions*. Weinheim, Germny: Wiley VHC Verlag, 2005. DOI: https://doi.org/10.1002/3527603492.

[10] J. Nierengarten, V. Gramlich, and F. Diederich, "Regio- and diasteroselective bisfunctionalization of c60 ande enantioselective synthesis of a c60 derivative with a chiral addition pattern," *Angew. Chem. Int. Ed. Eng*, vol. 35, no. 18, pp. 2101–2103, 1996. DOI: https://doi.org/10.1002/anie.19962101 .

[11] X. Camps and A. Hirsch, "Efficient cyclopropanation of C 60 starting from malonates," *J. Chem. Soc., Perkin Trans. 1*, vol. 97, pp. 1595–1596, 1997. DOI: https://doi.org/10.1002/anie.199621011.

[12] Y. He, H. Y. Chen, J. Hou, and Y. Li, "Indene - C60 bisadduct: A new acceptor for high-performance polymer solar cells," *J. Am. Chem. Soc.*, vol. 132, no. 4, pp. 1377–1382, 2010. DOI: https://doi.org/10.1021/ja908602j.

[13] E. Castro, J. Murillo, O. Fernandez-Delgado, and L. Echegoyen, "Progress in fullerene-based hybrid perovskite solar cells," *J. Mater. Chem. C*, vol. 6, no. 11, pp. 2635–2651, 2018. DOI: https://doi.org/10.1039/c7tc04302c.

[14] A. Montellano, T. Da Ros, A. Bianco, and M. Prato, "Fullerene C60 as a multifunctional system for drug and gene delivery," *Nanoscale*, vol. 3, no. 10, pp. 4035–4041, 2011. DOI: https://doi.org/10.1039/c1nr10783f.

[15] T. M. Figueira-Duarte *et al.*, "Synthesis and excited state properties of a [60]fullerene derivative bearing a star-shaped multi-photon absorption chromophore.," *Chem. Commun. (Camb).*, no. 19, pp. 2054–6, 2006. DOI: https://doi.org/10.1039/b601987k.

[16] W. Yan, S. M. Seifermann, P. Pierrat, and S. Bräse, "Synthesis of highly functionalized C60 fullerene derivatives and their applications in material and life sciences.," *Org. Biomol. Chem.*, vol. 13, no. 1, pp. 25–54, 2015. DOI: https://doi.org/10.1039/c4ob01663g.

[17] C. H. Chen, A. Aghabali, A. J. Metta-Magana, M. M. Olmstead, A. L. Balch, and L. Echegoyen, "Synthesis and characterization of a trans-1 hexakis-fullerene linker that forms crystalline polymers with silver salts," *Dalt. Trans.*, vol. 44, no. 42, pp. 18487–18491, 2015. DOI: https://doi.org/10.1039/c5dt03054d.

[18] M. Durka *et al.*, "The functional valency of dodecamannosylated fullerenes with Escherichia coli FimH--towards novel bacterial antiadhesives," *Chem. Commun.*, vol. 47, pp. 1321–1323, 2011. DOI: https://doi.org/10.1039/c0cc04468g.

[19] N. Tagmatarchis and H. Shinohara, "Fullerenes in medicinal chemistry and their biological applications.," *Mini Rev. Med. Chem.*, vol. 1, no. 4, pp. 339–48, 2001. DOI: https://doi.org/10.2174/1389557013406693.

[20] P. A. Troshin *et al.*, "Material solubility-photovoltaic performance relationship in the design of novel fullerene derivatives for bulk heterojunction solar cells," *Adv. Funct. Mater.*, vol. 19, no. 5, pp. 779–788, 2009. DOI: https://doi.org/10.1002/adfm.200801189.

[21] C. Tian, E. Castro, T. Wang, G. Betancourt-Solis, G. Rodriguez, and L. Echegoyen, "Improved performance and stability of inverted planar perovskite solar cells using fulleropyrrolidine layers," *ACS Appl. Mater. Interfaces*, vol. 8, no. 45, pp. 31426–31432, 2016. DOI: https://doi.org/10.1021/acsami.6b10668.

[22] C. Tian, K. Kochiss, E. Castro, G. Betancourt-Solis, H. Han, and L. Echegoyen, "A dimeric fullerene derivative for efficient inverted planar perovskite solar cells with improved stability," *J. Mater. Chem. A*, vol. 5, no. 16, pp. 7326–7332, 2017. DOI: https://doi.org/10.1039/c7ta00362e.

[23] Q.-Q. Ye, Z.-K. Wang, M. Li, C.-C. Zhang, K.-H. Hu, and L.-S. Liao, "N-type doping of fullerenes for planar perovskite solar cells," *ACS Energy Lett.*, vol. 3, no. 4, pp. 875–882, Apr. 2018. DOI: https://doi.org/10.1021/acsenergylett.8b00217.

[24] R. S. Ruoff, D. S. Tse, R. Malhotra, and D. C. Lorents, "Solubility of fullerene (C60) in a variety of solvents," *J. Phys. Chem.*, vol. 97, no. 13, pp. 3379–3383, 1993. DOI: https://doi.org/10.1021/j100115a049.

[25] N. Sivaraman, R. Dhamodaran, I. Kaliappan, T. G. Srinivasan, P. R. P. Vasudeva Rao, and C. K. C. Mathews, "Solubility of C70 in organic solvents," *Fuller. Sci. Technol.*, vol. 2, no. 3, pp. 233–246, Aug. 1994. DOI: https://doi.org/10.1080/15363839408009549.

[26] C. Bingel, "United States Patent [19]," 5,539,376, 1998.

[27] S. Ceola, L. Franco, M. Maggini, and C. Corvaja, "Optical spectrum of C60mono-adducts: Assignment of transition bands using time-resolved EPR magneto-photo-selection," *Photochem. Photobiol. Sci.*, vol. 5, no. 12, pp. 1177–1182, 2006. DOI: https://doi.org/10.1039/b610106b.

[28] T. O. Kyrey *et al.*, "Absorption characteristics of fullerene C 60 in N-methyl-2-pirrolidone/toluene mixture," *Fullerenes Nanotub. Carbon Nanostructures*, vol. 20, no. 4–7, pp. 341–344, 2012. DOI: https://doi.org/10.1080/1536383X.2012.655173.

[29] K. Hedberg, L. Hedberg, M. Bühl, D. S. Bethune, C. A. Brown, and R. D. Johnson, "Molecular structure of free molecules of the fullerene C70from gas- phase electron diffraction," *J. Am. Chem. Soc.*, vol. 119, no. 23, pp. 5314–5320, 1997. DOI: https://doi.org/10.1021/ja970110e.

[30] A. Herrmann, M. Ruttimann, C. Thilgen, and F. Diederich, "152. Chemistry of the Higher Fullerenes: Preparative isolation of C76 by HPLC and synthesis, separation, and characterization of Diels-Alder monoadducts of C70 and C76" *Helv. Chim. Acta*, vol. 77, no. 7, pp. 1689-1706, 1994. DOI: https://doi.org/10.1002/hlca.19940770703.

[31] M. J. Van Eis *et al.*, "Supramolecular fullerene chemistry: A comprehensive study of cyclophane-type mono- and bis-crown ether conjugates of C70," *Helv. Chim. Acta*, vol. 85, no. 7, pp. 2009–2055, 2002. DOI: https://doi.org/10.1002/1522-2675(200207)85:7<2009::AID-HLCA2009>3.0.CO;2-G.

[32] C. Thilgen and F. Diederich, "Chirality in fullerene chemistry," in *Topics in Stereochemistry*, Stuttgartt: John Wiley & Sons, 2003.

[33] M. R. Cerón *et al.*, "Tethered bis-pyrrolidine additions to C70: Some unexpected and new regioisomers," *Carbon N. Y.*, vol. 105, pp. 394–400, 2016. DOI: https://doi.org/10.1016/j.carbon.2016.04.044.

[34] A. Herrmann, M. Ruttimann, C. Thilgen, and F. Diederich, "125. multiple cyclopropanations synthesis and characterization of bis-, tris-, and tetrakis-adducts and chiroptical properties of bis-adducts with chiral addends, including a recommendation for the configurational description of fullerene derivatives with a chiral pattern," *Helv. Chim. Acta*, vol. 78, pp. 1673–1704, 1995. DOI: https://doi.org/10.1002/hlca.19950780705.

[35] T. Umeyama *et al.*, "Regioisomer effects of [70]fullerene mono-adduct acceptors in bulk heterojunction polymer solar cells," *Chem. Sci.*, vol. 8, no. 1, pp. 181–188, 2017. DOI: https://doi.org/10.1039/C6SC02950G.

[36] C. Reichardt and T. Welton, *Solvents and solvent effects in organic chemistry*. Weinheim, Germny: Wiley VHC Verlag, 2011.

[37] C. Thilgen and F. Diederich, *Higher Fullerenes: Covalent Chemistry and Chirality*. Heidelber, Berlin, Germany: Springer, 1999.

[38] F. Langa and P. de la Cruz, *Fullerenes: Principles and Aplications*. Cambridge, UK: RSC, 2007.

[39] E. Castro *et al.*, "New thiophene-based C60 fullerene derivatives as efficient electron transporting materials for perovskite solar cells," *New J. Chem.*, vol. 42, no. 17, pp. 14551–14558, 2018. DOI: https://doi.org/10.1039/C8NJ03067G.

[40] M. R. Cerón, M. Izquierdo, Y. Pi, S. L. Atehortúa, and L. Echegoyen, "Tether-directed bisfunctionalization reactions of C60 and C70," *Chem. – A Eur. J.*, vol. 21, no. 21, pp. 7881–7885, 2015. DOI: https://doi.org/10.1002/chem.201500206.

[41] E. Castro *et al.*, "A new family of fullerene derivatives: fullerene-curcumin conjugates for biological and photovoltaic applications," *RSC Adv.*, vol. 8, no. 73, pp. 41692–41698, 2018. DOI: https://doi.org/10.1039/C8RA08334G.

[42] A. Cabrera-Espinoza, B. Insuasty, and A. Ortiz, "Novel BODIPY-C60 derivatives with tuned photophysical and electron-acceptor properties: Isoxazolino[60]fullerene and pyrrolidino[60]fullerene," *J. Lumin.*, vol. 194, pp. 729–738, 2018. DOI: https://doi.org/https://doi.org/10.1016/j.jlumin.2017.09.043.

[43] "Cyclic Voltammetry of Fullerene Derivatives and Bilayer Devices," 02, 02, 2021. [Online]. Available: http://www-solar.materials.ox.ac.uk/uploads/images/theses/6. C-V BEAL.pdf.

[44] Y. Fang, C. Bi, D. Wang, and J. Huang, "The functions of fullerenes in hybrid Perovskite solar cells," *ACS Energy Lett.*, vol. 2, no. 4, pp. 782–794, Apr. 2017. DOI: https://doi.org/10.1021/acsenergylett.6b00657.

[45] C.-H. Chiang, Z.-L. Tseng, and C.-G. Wu, "Planar heterojunction perovskite/PC71BM solar cells with enhanced open-circuit voltage via a (2/1)-step spin-coating process," *J. Mater. Chem. A*, vol. 2, no. 38, pp. 15897–15903, 2014. DOI: https://doi.org/10.1039/C4TA03674C.

[46] S.-M. Dai *et al.*, "Formulation engineering for optimizing ternary electron acceptors exemplified by isomeric PC71BM in planar perovskite solar cells," *J. Mater. Chem. A*, vol. 4, no. 48, pp. 18776–18782, 2016. DOI: https://doi.org/10.1039/C6TA07750A.

[47] Y. Shao, Y. Yuan, and J. Huang, "Correlation of energy disorder and open-circuit voltage in hybrid perovskite solar cells," *Nat. Energy*, vol. 1, no. 1, p. 15001, 2016. DOI: https://doi.org/10.1038/nenergy.2015.1.

[48] S. Few, J. Frost, and J. Nelson, "Models of charge pair generation in organic solar cells," *Phys. Chem. Chem. Phys.*, vol. 17, no. 4, pp. 2311–2325, 2015. DOI: https://doi.org/10.1039/C4CP03663H.

[49] P. Morvillo and E. Bobeico, "Tuning the LUMO level of the acceptor to increase the open-circuit voltage of polymer-fullerene solar cells: A quantum chemical study," *Sol. Energy Mater. Sol. Cells*, vol. 92, no. 10, pp. 1192–1198, 2008. DOI: https://doi.org/10.1016/j.solmat.2008.04.010.

[50] O. Fernandez-Delgado *et al.*, "Variation of interfacial interactions in PC61BM-like electron-transporting compounds for perovskite solar cells," *ACS Appl. Mater. Interfaces*, vol. 11, no. 37, pp. 34408–34415, 2019. DOI: https://pubs.acs.org/doi/10.1021/acsami.9b09018.

Article citation:
A. Duarte-Ruiz, H. Iuele, S. A. Torres-Cortés, A. Meléndez, J. D. Velásquez & M. N. Chaur, "Synthesis and characterization of C_{60} and C_{70} acetylacetone monoadducts and study of their photochemical properties for potential application in solar cells", Rev. Colomb. Quim., vol. 50, no. 1, pp. 86-97, 2021. DOI: https://doi.org/10.15446/rcq.v50n1.88545